Inflammopharmacology (2023) 31:2751–2771
https://doi.org/10.1007/s10787-023-01313-x

Inflammopharmacology

ORIGINAL ARTICLE

Voglibose attenuates cognitive impairment, Aβ aggregation, oxidative stress, and neuroinflammation in streptozotocin-induced Alzheimer's disease rat model

Manickam Rajkumar[1] · Soundarapandian Kannan[1] · Ramasundaram Thangaraj[2]

Received: 2 August 2023 / Accepted: 7 August 2023 / Published online: 4 September 2023

Abstract

Alzheimer's disease (AD) is an age-dependent neurodegenerative disease hallmarked by Amyloid-β (Aβ) aggregation, cognitive impairment, and neuronal and synaptic loss. In this study, AD was induced in male Wistar rats ($n=6$) by the administration of intracerebroventricular-streptozotocin (ICV-STZ-3 mg/kg/day), and Voglibose (Vog) was administered at various doses (10, 25, and 50 mg/kg), while Galantamine (3 mg/kg) acted as a reference standard drug. Behavioral alterations in both spatial and non-spatial memory functions were evaluated in the experimental rats. At the end of the study, all experimental rats were sacrificed, and their brain parts, the cortex and hippocampus, were subjected to biochemical, western blot, and histopathological analysis. In our study results, the statistically significant dose-dependent results from the behavioral tests show the Voglibose-treated groups significantly improved ($p<0.0001$) spatial and non-spatial memory functions when compared with ICV-STZ-treated group. Meanwhile, when compared with ICV-STZ-treated rats, treatment with Voglibose (10, 25, and 50 mg/kg) showed the activities of both acetylcholinesterase (AChE) and malondialdehyde (MDA) were significantly attenuated ($p<0.0001$), while the operation of antioxidant enzymes was considerably enhanced ($p<0.0001$). The molecular estimation showed that it significantly attenuates ($p<0.0001$) the TNF-α, IL-1β, and CRP activity, and the western blot results demonstrate the significantly attenuated Aβ aggregation. The histopathological results showed that the Voglibose treatment had an effective improvement in clear cytoplasm and healthy neuronal cells. In conclusion, our results suggest that Voglibose has potent neuroprotective effects against the ICV-STZ-induced AD model. Furthermore, these results support the possibility of Voglibose as a therapeutic approach to improving cognitive function, suggesting that controlling Aβ aggregation might be a novel target for the development of AD.

Keywords Alzheimer's disease · Voglibose · Streptozotocin · Aβ aggregation · Oxidative stress

Introduction

Alzheimer's disease (AD) is a type of neurodegenerative disease that leads to a gradual loss of memory and is one of the most common causes of dementia (Malik et al. 2022). A report from 2017 suggests that approximately 44 million individuals worldwide are affected by AD, and this number could increase to 115 million by the year 2050 (Alzheimer's Association 2017). AD is characterized by specific pathological features such as the deposition of amyloid beta (Aβ) aggregation, oxidative stress, the formation of neurofibrillary tangles within the cells, neuroinflammation, and the subsequent loss of neurons and synapses, resulting in cognitive deficits (Leng and Edison 2021; Sajad et al. 2022). Recent studies have identified that type 2 diabetes mellitus, obesity, and other pre-diabetic conditions of insulin resistance may increase the risk factors for AD. Central insulin resistance is the failure of the brain cells to respond to insulin and can occur due to several factors like downregulation of insulin receptors, inability to bind insulin receptors with insulin, or defective activation of the insulin signaling cascade (Rodrigues et al. 2020). Research indicates that insulin receptor density decreases with age, and a decrease in insulin mRNA

✉ Soundarapandian Kannan
skperiyaruniv@gmail.com

[1] Cancer Nanomedicine Laboratory, Department of Zoology, School of Life Sciences, Periyar University, Salem, Tamil Nadu 636 011, India

[2] Department of Zoology, Periyar University, Salem, Tamil Nadu 636 011, India

expression in postmortem brain tissues of AD patients signifies a lack of this hormone in the brain. Additionally, central insulin resistance results in reduced downstream signaling through the inhibition of the phosphorylation of PI3K and Akt, leading to increased activation of GSK-3β, thereby contributing to the pathogenesis of AD (Akhtar et al. 2020a, b).

Voglibose (Vog) is a α-glucosidase inhibitor (α-GI) that helps to control postprandial hyperglycemia (PPHG) by inhibiting the glucose-hydrolyzing enzyme α-glucosidase (maltase) and reducing carbohydrate absorption. This drug is commonly used to treat type 2 diabetes patients and has been shown to control blood glucose levels by inhibiting insulin receptors in numerous studies (Moritoh et al. 2010; Jayant et al. 2016). Inflammatory responses and their mediators play a crucial role in the onset of neurodegenerative diseases, making it essential to study cerebrum protective agents that can slow down the disease's progression. Voglibose has emerged as a potential candidate in this regard, as studies conducted on animal models have reported its beneficial effects (Kim et al. 2019). For instance, Voglibose administration can lead to a reduction in stress and cognitive dysfunction in rats with chronic activity-related diabetes and MCAo-induced ischemic stroke, thus attenuating the anti-stroke activity (Shah et al. 2020). On the other hand, Voglibose has been studied for oxidative stress and some other related diseases (Derosa et al. 2012). But its potential effects on amyloid neuropathy, oxidative stress, cholinesterase inhibitors, energy metabolism deficiencies, and inflammation remain relatively unexplored.

Streptozotocin (STZ) is a compound containing glucosamine-nitrosourea that modifies glucose metabolism, insulin signaling, protein kinases, synaptic function, and induces brain cell apoptosis when administered through the intracerebroventricular (ICV) injection method (Agrawal et al. 2020). In addition, it causes cognitive impairment, increased cerebral aggregates of Aβ fragments, and hyperphosphorylation of tau protein. These changes are accompanied by a reduced glycogen synthase kinase (GSK-3) alpha/beta ratio, indicative of pathophysiological changes such as cholinergic and insulin receptor dysfunction, energy metabolism impairment, tau hyperphosphorylation, and oxidative stress (Salkovic-Petrisic et al. 2013). ICV-STZ administration also produces cholinergic deficits, oxidative stress, and neuroinflammation in the brain, making it a popular model to explore the pathophysiological mechanisms of central insulin resistance-induced AD. Consequently, rats with ICV-STZ-induced cognitive deficits have been proposed as a research model for understanding AD (Akhtar et al. 2020a, b).

Oxidative stress is involved in a variety of diseases, including chronic inflammation and AD. The brain's neurons have high energy production and oxygen consumption rates, making them particularly vulnerable to overproduction of reactive oxygen species (ROS) and subsequent oxidative damage. Brain regions that regulate cognitive and motor function, such as the hippocampus (HS) and cortex (CS), are more prone to oxidative stress, and therefore require antioxidants (Leyane et al. 2022; Tirichen et al. 2021). Therefore, antioxidant therapy has been proposed as a means of preventing and treating AD. Additionally, neuroinflammation is thought to play a significant role in AD pathogenesis, characterized by glial activation and the release of inflammatory mediators that fuel a cycle of neuroinflammatory attacks (Tezel 2022). Inflammatory cytokines like tumor necrosis factor-α (TNF-α) and interleukin (IL)-1β can further activate glial cells, affecting cognitive and memory functions. Comparatively, the ICV-STZ-induced model is more suitable for studying AD-related neuroinflammation, as evidenced by a study between ICV-STZ-induced rats (Agrawal et al. 2020). ICV-STZ-treated animals also display cholinergic deficiency, as evidenced by increased acetylcholinesterase (AChE) activity in the HS. Hence, inhibiting AChE to enhance cholinergic activity is another potential treatment method for AD (Yamini et al. 2022).

The role of mitochondrial dysfunction in the development of AD has gained attention. This dysfunction entails changes in mitochondrial electron transfer chain complex activities that lead to oxidative stress and subsequent neuronal apoptosis, thereby contributing to the pathophysiology of AD (Cheng et al. 2020). It has been observed that excitotoxicity, among other factors, predisposes neurons to damage associated with age-related AD. Further, AD is the accumulation and aggregation of extracellular amyloid-β (Aβ), which arises from an imbalance between Aβ generation and clearance. Recent evidence suggests that impaired Aβ clearance commonly precedes the development of AD (Gallego Villarejo et al. 2022). Therefore, the efficient removal of brain-derived Aβ while overcoming the blood–brain barrier (BBB) is a highly promising therapeutic approach for AD (Ma et al. 2021). Interestingly, peripheral Aβ clearance has been shown to trigger a large Aβ efflux from the brain to the periphery, leading to a significant decrease in cerebral Aβ levels. As a result, peripheral Aβ clearance has been proposed as a novel approach to overcoming the BBB challenge and eliminating brain-derived Aβ. Numerous therapeutic strategies for clearance of peripheral Aβ have made strides in AD treatment (Xue, et al. 2022; Ma et al. 2021). However, in many cases, these therapeutic agents promote the aggregation of Aβ, inducing cytotoxicity and cell death due to increased local Aβ concentrations resulting from Aβ accumulation on material surfaces. Developing a targeted therapy for the peripheral system that can effectively control the progression of AD is crucial (Sanchez-Rodriguez et al. 2023). However, the FDA-approved drugs for the treatment of AD are cholinomimetics such as rivastigmine, Galantamine, and donepezil (Kareem et al. 2021). However, there

remains a scarcity of clinically effective therapeutic drugs for AD. Further, to the best of our knowledge, no one has yet investigated the therapeutic potential of AD using Voglibose in cognitive deficits, Aβ aggregation, oxidative stress, and neuroinflammation.

The novelty of this present study was the examination of Voglibose drug (10, 25, and 50 mg/kg) as a therapeutic target for the treatment of AD. This study aimed to investigate the Voglibose drug treated with ICV-STZ-induced AD experimental rats' spatial and non-spatial cognitive memory functions. Further, we designed to investigate the potential role of Voglibose against ICV-STZ-induced Aβ aggregation and oxidative stress. This study evaluated the effect of Voglibose on ICV-STZ-mediated neurodegeneration, mitochondrial dysfunctions, neuroinflammation, histological changes, and cholinergic functions for the clinical application of AD.

Materials and methods

Animals

Adult male Wistar rats weighing 200 ± 10 gm, of breed, in the Central Animal House facility of Periyar University, Salem, Tamil Nadu, India, were used in this study. In the present study, each live specimen or specimen group ($n = 6$ for each investigated group) was subjected to several experiments. The experimental animals were contained in a polycarbonate cage with three individuals in each, under conditions of regular feeding on standardized feed pellets and water, in a room with a 12-h light/12-h dark cycle and a continuous temperature of 22–25 °C and humidity of 45–55 °C. All experimental protocols were performed as per the suggestion of the Ministry of Fisheries, Animal Husbandry, and Committee for the Purpose of Control and Supervision of Experiments on Animals (CPCSEA), Government of India, and the experimental procedures followed have been approved by the Institutional Animal Ethical Committee (PU-IAEC/2020/M1/19), Periyar University, Salem, Tamil Nadu, India. Efforts have been made to decrease animal distress, and the lowest number of animals was used for the experiments to validate the statistical significance of the data.

Drugs and treatment

Voglibose, Galantamine, and streptozotocin were purchased from Sigma-Aldrich (MS, USA). Streptozotocin was dissolved in artificial cerebrospinal fluid (aCSF) with a composition of 2.9 mM KCl, 1.7 mM $CaCl_2$, 147 mM NaCl, 1.6 mM $MgCl_2$, and 2.2 mM MD-glucose. On the other hand, Voglibose was dissolved in double-distilled water. Freshly prepared drug solutions were administered to rats at doses of Voglibose (10, 25, and 50 mg/kg) and Galantamine (3 mg/kg) over 14 days using stereotaxic apparatus. The other chemicals used in this study were of analytical grade (Sharma et al. 2015).

Experimental design

Rats were randomly divided into six groups, each group having six animals. Group I: (Control): Normal saline (CSF); Group-II: STZ + CSF (3 mg/kg); Group III: STZ + Gal (3 mg/kg/day); Group IV: STZ + Vog (10 mg/kg/day); Group V: STZ + Vog (25 mg/kg/day); Group VI: STZ + Vog (50 mg/kg/day). Each rat received the specified drug solution through stereotaxic apparatus. Behavioral experiments, including the open-field test to evaluate locomotor activity and the Morris water maze (MWM), passive avoidance (PA), and Y-maze test to assess spatial and non-spatial memory, were then conducted to gauge the rats' learning and memory functions. The experimental design is shown in Fig. 1.

Intracerebroventricular-streptozotocin (ICV-STZ) injection

The procedure for the ICV-STZ injection was conducted using the method described in Yamini et al. (2018). The rats underwent anesthesia using ketamine hydrochloride (80 mg/kg, i.p.) + xylazine (10 mg/kg, i.p.). The rat's scalp was shaved, and it was positioned in a stereotaxic apparatus. A midline sagittal incision was made in the scalp, and burr holes were created on both sides of the skull over the lateral ventricles using the following coordinates: 0.8 mm posterior to the bregma, 1.5 mm lateral to the sagittal suture, and 3.6 mm beneath the cortical surface of the brain (Paxinos et al. 1980). Bilateral injections of freshly prepared STZ (3 mg/kg) were administered on the 1 and 3 days in two divided doses of 1.5 mg/kg each day after being dissolved in aCSF. Following each injection, the wound was sutured, and the application of antiseptic powder (Neosporin) was made. As for the control group, ICV injections of the same volume of aCSF were given on the 1st and 3rd days. The experimental rats were given water and a normal pellet diet daily.

Behavioral assessments

Morris water maze (MWM) test

The MWM test was mainly used to examine physical activity and spatial memory, as described in Morris (1984). Briefly, a circular black pond (160 cm in diameter and 70 cm in height) was filled with water to a depth of 40 cm and maintained at a temperature of 25 ± 2 °C, also made opaque with

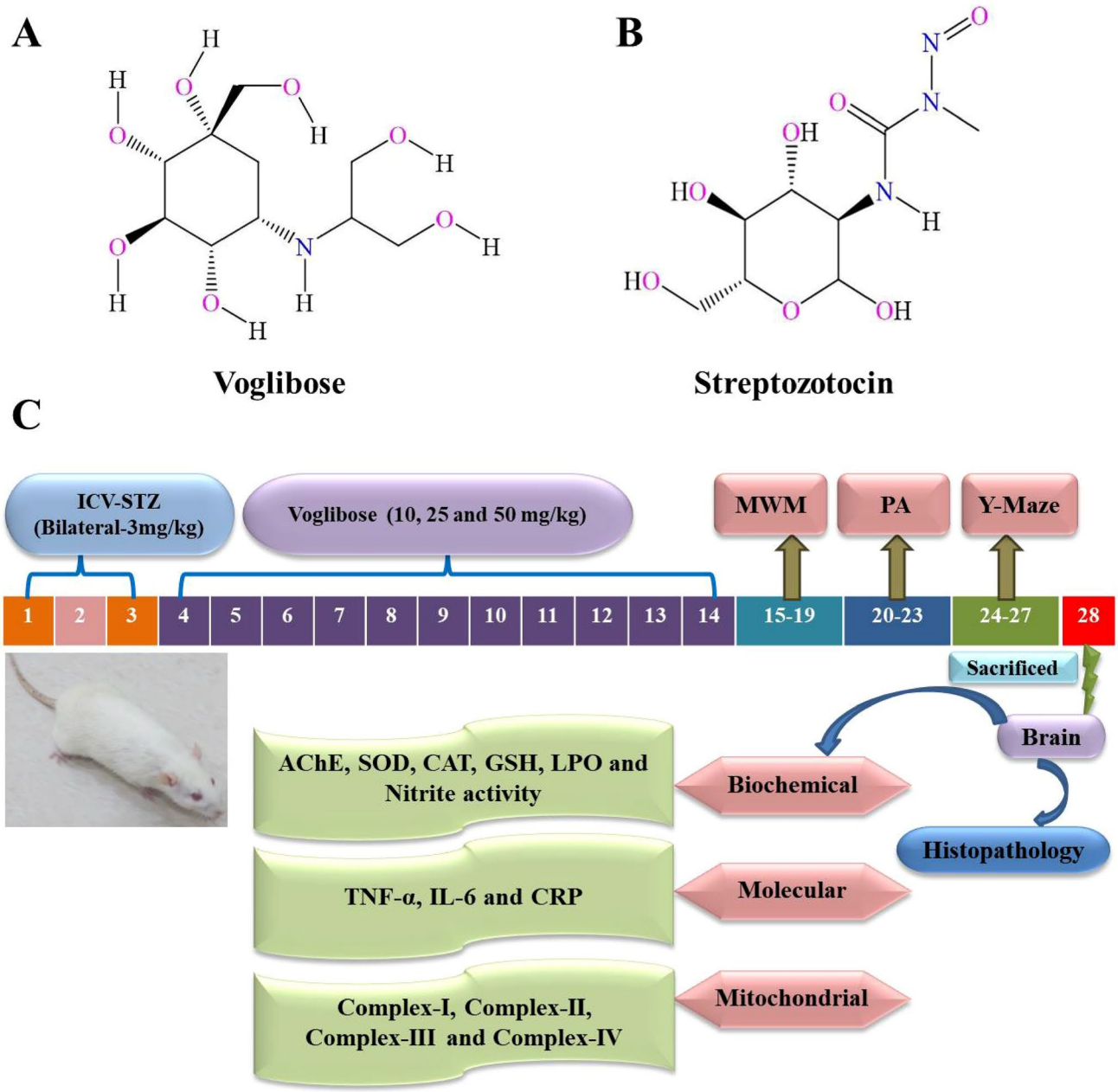

Fig. 1 Diagram of the experimental procedure and group assignment *ICV-STZ* intracerebroventricular-streptozotocin, *MWM* Morris water maze, *PA* passive avoidance, *AChE* acetylcholinesterase, *SOD* superoxide dismutase, *CAT* catalase, *GSH* reduced glutathione, *LPO* lipid peroxidation, *TNF-α* tumor necrosis factor alpha, *IL-6* interleukin 1 beta, *CPR* C-reactive protein

white paint. A platform (10 cm in diameter) was placed 2 cm below (hidden) or above (visible) the surface of the water ($n=6$). In the MWM pool, a digital video camera was set up to record the animals' locomotion activity. The MWM task was conducted for 5 days, with animals undergoing a set of experimental procedures. For each procedure, 30-min intervals were followed. All rats were trained with four trails per day, each with a different starting point in the pool (A, B, C, and D), and the escape latency was measured with a stopwatch, with a maximum of 60 s allowed for each trail. All the experimental rats' visual and motor performances were recorded, and the percentage of escape latency, time spent in the target quadrant, error time, and swimming speed were determined.

Passive avoidance (PA) task

The PA experimental protocol was conducted as previously described (Ramagiri and Taliyan 2017). To conduct the step-through passive avoidance test, the equipment used comprised a compartment (25 × 21 × 25 cm), which was illuminated, and a dark compartment of the same size. These two compartments were separated by a wall that had a guillotine door. The rat was trained in this apparatus, where they were initially placed in the illuminated compartment, facing away from the dark one, and allowed free access for 3 min per day for 4 consecutive days. On all experimental days, during the learning session, the rats were once again placed in the same compartment, and the rats entered the dark room, a 0.5 mA electric shock was delivered through the grid platform for 3 s, and the door was automatically closed to confine them into the dark compartment. Mice remained in the dark chamber for 10 s and then returned to their home cage. In the following days, the rats were again placed in the illuminated compartment, and the time taken to enter the dark compartment and the number of times they stepped inside the dark compartment was maximum recorded and evaluated for 300 s.

Y-maze test

The Y-maze experimental procedure was conducted as previously described (Conrad et al. 1996). Each arm of the maze was 40 cm in length, 15 cm high, and 15 cm wide, and was composed of black Plexiglas. The arms are convergent in a central equilateral triangular region with a 15 cm longest axis. The procedure was as follows: each rat was given one arm at the end of the other and allowed to cruise the maze generously for a maximum of 5 min. The sequence of arm entries was visually recorded. When the foundation of the rat tail was completely within the arm, the entry was examined completely. A consecutive entrance for three arms (A, B, and C) overlapping into the triplet sets was characterized as an alternation. As the total number of arms approached 2 min, the maximum number of feasible spontaneous alternations was calculated, and the percentage was calculated as the ratio of actual to possible alternations × 100.

Biochemical measurements

Dissection and homogenization

The experimental rats were divided into two groups following final behavioral assessments (Sharma et al. 2015). The first group was utilized for biochemical experiments, whereas the second group was used for histopathological analysis using hematoxylin and eosin stains. The cortex (CS), as well as the hippocampus (HS), were dissected and homogenized (10% w/v) in ice-cold PBS (PBS, 0.1 M, pH 7.4). A homogenate was prepared by centrifugation at 10,000*g* for 15 min at 4 °C and used for the oxidative-nitrosamine biochemical assay. The biochemical investigation was estimated using a double-beam UV–Vis spectrophotometer [UV-1800 Shimadzu (Japan)].

Estimation of AChE activity

AChE activity (a cholinergic neuron marker in the brain) was assessed in the CS and HS regions described in the previous method (Ellaman et al. 1961). The mixture for the assay contained 0.05 ml of homogenate, 0.01 M sodium phosphate buffer (pH 8), 0.10 ml of acetylcholine iodide, and 0.10 ml of DTNB (Ellman's reagent). The changes in absorbance values were measured at 412 nm for 5 min. The results were calculated using the molar extinction coefficient of the chromophore (1.36×10^4 M cm^{-1}) used to calculate the result at hydrolyzed/min/mg of protein.

Estimation of superoxide dismutase (SOD) activity

The SOD activity was analyzed according to the previous method (Kono 1978). The rat brain parts were homogenized in ice-cold 50 mM PBS (pH 7.0) containing 0.1 mM EDTA to yield a 5% homogenate (w/v). Homogenates were centrifuged at 10,000*g* for 10 min at 4 °C using a cooling centrifuge. Approximately 100 µl of tissue homogenate was mixed with 880 µl of carbonate buffer (0.05 M, pH 10.2, containing 0.1 mM EDTA) and added to the mixture with 20 µl of 30 mM epinephrine (0.05% acetic acid), and the optical density values at 480 nm were measured using a UV–Vis spectrophotometer. The SOD activity was measured as the amount of enzyme inhibiting epinephrine's oxidation by 50%, which is 1 unit of activity. The results were represented as Units/mg of protein, with 1 U of an enzyme equaling the total amount of enzyme that completely inhibits the rate of reaction by 100%.

Estimation of catalase (CAT) activity

The CAT activity was analyzed following the method (Claiborne 1985). The rat brain regions were homogenized in ice-cold PBS (50 mM, pH 7.0) containing EDTA at 0.1 mM to provide 5% homogenate (w/v). Homogenates were centrifuged at 10,000*g* for 10 min at 4 °C using a cooling centrifuge. Homogenate from the centrifuge was taken in the amount of 100 µl, and 10 µl of 100% ethyl alcohol was added and the samples were maintained in an ice bath for 30 min. After 30 min, allowing the tubes to warm to room temperature, 10 µl of Triton X-100 RS was added to every tube. In a

cuvette containing 50 µl of homogenate, 200 µl of PBS and 250 µl of 0.066 M H_2O_2 were added after optical density was determined at 240 nm for 60 s in a UV–Vis spectrophotometer. Absorbance values were determined, and the results were expressed as µM of H_2O_2 decomposed/min/mg protein.

Estimation of glutathione (GSH) level

The GSH content in the CS and HS regions, with slight modifications, was measured according to the previous method (Jollow et al. 1974). Briefly, the rat brain regions were mixed with 4% sulfosalicylic acid (w/v) in a 1:1 ratio, incubated for 1 h at 4 °C, and then samples were immediately centrifuged at 1200 *g* for 15 min at 4 °C. Briefly, an assay mixture containing 0.1 ml of supernatant, 0.1 M PBS (pH 7.4), and 1.0 mM DTNB was prepared. The prepared sample's yellow color was immediately measured using a UV–Vis spectrophotometer at 412 nm. The GSH content was calculated as nmol, using the molar extinction coefficient of the chromophore as 13.6×10^3 M^{-1} cm^{-1}.

Measurement of lipid peroxidation (LPO) assay

The LPO activity was analyzed according to the previous method (Wills 1966). To assess oxidative stress through lipid peroxidation, malondialdehyde (MDA) is used as an indicator. To conduct the LPO assay, 100 µl of tissue homogenate supernatant was mixed with 100 µl of 0.1 M Tris–HCl (pH 7.4) and then incubated at 37 °C for 2 h. Following this, 200 µl of 10% TCA was added to the mixture, and the resulting solution was centrifuged at 1000 *g* for 10 min. 200 µl of supernatant was added to 200 µl (0.67% w/v) of thiobarbituric acid (TBA) and mixed well. The samples were then kept in boiling water for 10 min, resulting in the production of pink color. The solution was cooled, and 200 µl of distilled water was added to it before measuring the absorbance at 532 nm on a UV–Vis spectrophotometer. Calculations were performed, and the results were expressed in terms of nmol/MDA/mg of protein.

Estimation of nitrite activity

Nitric oxide is a short-lived substance that undergoes spontaneous oxidation to form nitrite and nitrate. To estimate plasma nitrite levels, the methodology described by previous methods was followed (Green et al. 1982). For the nitrite assay, equal volumes of 100 µl of tissue homogenate sample and 100 µl of Griess reagent (0.1% *N*-(1-naphthyl)-ethylenediamine dihydrochloride + 1% sulfanilamide in 5% phosphoric acid) were mixed. This mixture was then kept in a dark room and incubated at 25–30 °C for 10 min. The absorbance of the solution was measured at 540 nm using a UV–Vis spectrophotometer, and nitrite concentrations were interpreted from a standard curve of sodium nitrite solution. Finally, the results were expressed as nmol/nitrite/mg of protein.

Estimation of glutathione peroxidase (GPx) activity

To estimate GPx activity, it was assayed according to the previous method (Lawrence et al. 1976). Briefly, a mixture of 2 ml was prepared consisting of 1.44 ml of 0.5 M phosphate buffer (pH 7.0), 100 µl of 1 mM EDTA, 100 µl of 1 mM sodium azide, 50 µl of glutathione reductase (1 EU/ml), 100 µl of 1 mM glutathione, 100 µl of 2 mM NADPH, and 10 µl of 0.25 mM hydrogen peroxide (H_2O_2). 100 µl of the tissue supernatant sample was added to this mixture, and absorbance measurements were immediately evaluated at 340 nm for 2 min at 60-s intervals. The absorbance change was recorded, and the calculated values were expressed in terms of nM of oxidized NADPH/min/mg of protein using a molar extinction coefficient of 6.22×10^3 M^{-1} cm^{-1}.

Mitochondrial estimation

Isolation of mitochondria

To isolate mitochondria, the CS and HS regions were dissected from a rat brain following the previous method (Berman and Hastings 1999). Initially, the tissue was homogenized in ice-cold isolation buffer (containing 75 mM sucrose, 215 mM mannitol, 0.1% BSA, 20 mM HEPES, 1 mM EGTA, and pH 7.2) with EGTA. The homogenates were then centrifuged at 1000 *g* for 5 min at 4 °C, and the resulting pellets were resuspended in the isolation buffer with EGTA. The samples were then resuspended at 13,000 *g* for 5 min at 4 °C. The resulting homogenate was transferred, topped off with isolation buffer with EGTA, and spun once more at 13,000 *g* for 10 min at 4 °C. Pellets were resuspended in an isolation buffer with EGTA, incubated with 1 ml of digitonin for 10 min, and then resuspended at 13,000 *g* for 10 min at 4 °C. The final pellets containing pure mitochondria were resuspended in an isolation buffer without EGTA.

NADH dehydrogenase activity (complex I)

Nicotinamide adenine dinucleotide (NADH) dehydrogenase activity in the CS and HS was analyzed using a previous method (King and Howard 1967). In this method, NADH is catalytically oxidized to NAD^+ followed by the reduction of cytochrome C. The reaction mixture consisted of NADH (6 mM), cytochrome C (10.5 mM), and glycyl glycine buffer

(0.2 M, pH 8.5). To initiate the reaction, a required quantity of solubilized mitochondrial homogenate was added, and the changes in absorbance at 550 nm were recorded over 3 min at 1 min intervals using a UV–Vis spectrophotometer. The results were then expressed as nmol of NADH oxidized/min/mg of protein.

Succinate dehydrogenase activity (complex II)

Succinate dehydrogenase activity in the CS and HS was measured according to the previous method (King and Howard 1967). This involved oxidizing succinate with an artificial electron acceptor, potassium ferricyanide. To initiate the reaction, a mitochondrial sample was added to a reaction mixture containing phosphate buffer (0.2 M), succinic acid (0.6 M), 1% BSA, and potassium ferricyanide (0.03 M) at pH 7.8. The change in absorbance was measured at 420 nm at intervals of 1 min for 3 min. The activity was expressed as nmol of substrate/min/mg of protein.

3-(4,5-Dimethylthiazol-2-yl)-2,5-diphenyltetrazolium bromide (MTT) ability (complex III)

This method is an indirect technique utilized to measure the activity of complex III. As per the previous method (Mosmann 1983), a pale yellow MTT substrate is incubated with mitochondrial samples. Upon incubation, a purple product is produced, which can be solubilized with dimethyl sulfoxide (DMSO) and measured to determine the number of viable cells/well. In general, each well is filled with 10 µl of MTT and incubated for 3 h at 37 °C in a humidified atmosphere containing 5% CO_2 and 95% air. The medium is then aspirated and lysed with 50% DMSO. The absorbance of the resulting medium is measured at a wavelength of 580 nm using an ELISA reader. The quantified data are directly proportional to the product resulting from the incubation with MTT.

Cytochrome-c oxidase assay (complex IV)

To estimate the amount of cytochrome-c oxidase (complex IV), a mixture was formed by combining 100 µl of 0.3 mM reduced cytochrome-c (reduced using sodium borohydride crystals, pH adjusted to 7.0 by 100 mM HCL) and 700 µl of 75 mM phosphate buffer. To initiate the reaction, 10 µl of a mitochondrial sample was added, and the absorbance was immediately recorded at 550 nm for 180 s at intervals of 60 s. The obtained readings were used for calculations, and the results were expressed in terms of the nmole of cytochrome-c oxidized/min/mg of protein, as per the method described by Sottocasa et al. (1967).

Estimation of TNF-α, IL-6, and CRP levels

To estimate the levels of Tumor Necrosis Factor Alpha (TNF-α), Interleukin-6 (IL-6), and C-reactive protein (CRP) in hippocampal homogenate, an enzyme-linked immunosorbent assay (ELISA) was performed as per the instructions provided by the manufacturer kit (Yamini et al. 2018). The respective standard curves were used to determine the quantity of TNF-a, IL-6, and CRP present in the hippocampal tissue homogenate. The results were expressed as mean ± SD, with TNF-a, and IL-6 expressed as pg/mg protein and CRP expressed as ng/mg protein, respectively.

Western blot analysis

CS and HS tissues were homogenized in cold RIPA buffer. Using a BCA protein assay kit, the protein concentration was calculated (Hatai et al. 2017). Briefly, protein extracts (30 g per lane) from the CS and HS were separated by 10–12% sodium dodecyl sulfate–polyacrylamide gel electrophoresis and then electrophoretically transferred onto the PVDF membrane. After being blocked with 5% skimmed milk and overnight incubated with respective primary antibodies, including Aβ and β-Actin (Santa Cruz Biotechnology, Santa Cruz, CA). Membranes were exposed to the appropriate secondary antibodies for 1 h. Protein band separations were visualized using enhanced chemiluminescence to identify reagents (ECL, Millipore). As a loading control, β-actin (1:5000) was used. With the use of a chemiluminescent substrate, protein bands were found (Thermo). To account for variations in sample loading and transfer, the densitometry values of protein bands were normalized to β-actin immunoreactivity.

Histopathological analysis

After the last experimental day, all the experimental rats were sacrificed using ketamine (80 mg/kg, i.p.) + xylazine (10 mg/kg, i.p.) by decapitation immediately. Decapitated animal parts such as the brain (CS and HS), heart, liver, kidney, and lung were fixed in 10% paraformaldehyde for 5 h. The tissue was then dehydrated and histologically processed. Then they remained surrounded by paraffin wax, were cut into 3-µm-thick sections, and stained with hematoxylin and eosin. The stained slides were examined at lower-than-bright field illumination using AHBT-51 (Olympus Vanox Research Microscope, Japan) light microscopy through a 40 × objective lens. A histological examination of vital organs was carried out to see if the degradation of Voglibose-treated development and any pathologic impacts such as

necrosis or inflammation had occurred in experimental rats (Ahn et al. 2017; Mishra et al. 2018).

Protein estimation

Protein estimation was done by following Lowry's method using the standard bovine serum albumin (Lowry et al. 1951).

Statistical analysis

All statistical analysis was done with Graph Pad Prism (Graph Pad Prism Software, San Diego, CA, USA). Statistical analysis for behavioral assessment was evaluated by two-way analysis of variance (ANOVA), followed by Bonferroni's post hoc test for multiple comparisons. One-way ANOVA was used to analyze the biochemical data, followed by Tukey's test for multiple comparisons. Data were expressed as the mean ± standard deviation (mean ± SD), and the results were calculated to be significantly different from the $p < 0.05$.

Results

Behavioral assessment

Effect of Vog on MWM test

During the MWM test, cognitive function was evaluated. The mean escape latency was found to be similar across all the groups on the initial day of testing. However, from the 2nd day onwards, a noteworthy difference in escape latency was observed. ICV-STZ rats exhibited a decreased ability to locate and learn the position of the platform on the 4th and 5th days of training, as shown in Fig. 2B. However, this impaired performance was significantly attenuated [($F_{(5,24)} = 139.8$, $R^2 = 0.9148$ ($p < 0.0531$)] by chronic treatment with 10, 25, and 50 mg/kg of Vog and 3 mg/kg of Gal. This treatment with 50 mg/kg showed a significantly decreased ($p < 0.0001$) escape latency required to locate the platform on the 5th day of the training period. The time spent in the target quadrant (TSTQ) and swimming path length was found to decrease significantly [($F_{(5,30)} = 94.96$, $R^2 = 0.9406$ ($p < 0.0001$)] in the ICV-STZ group as compared

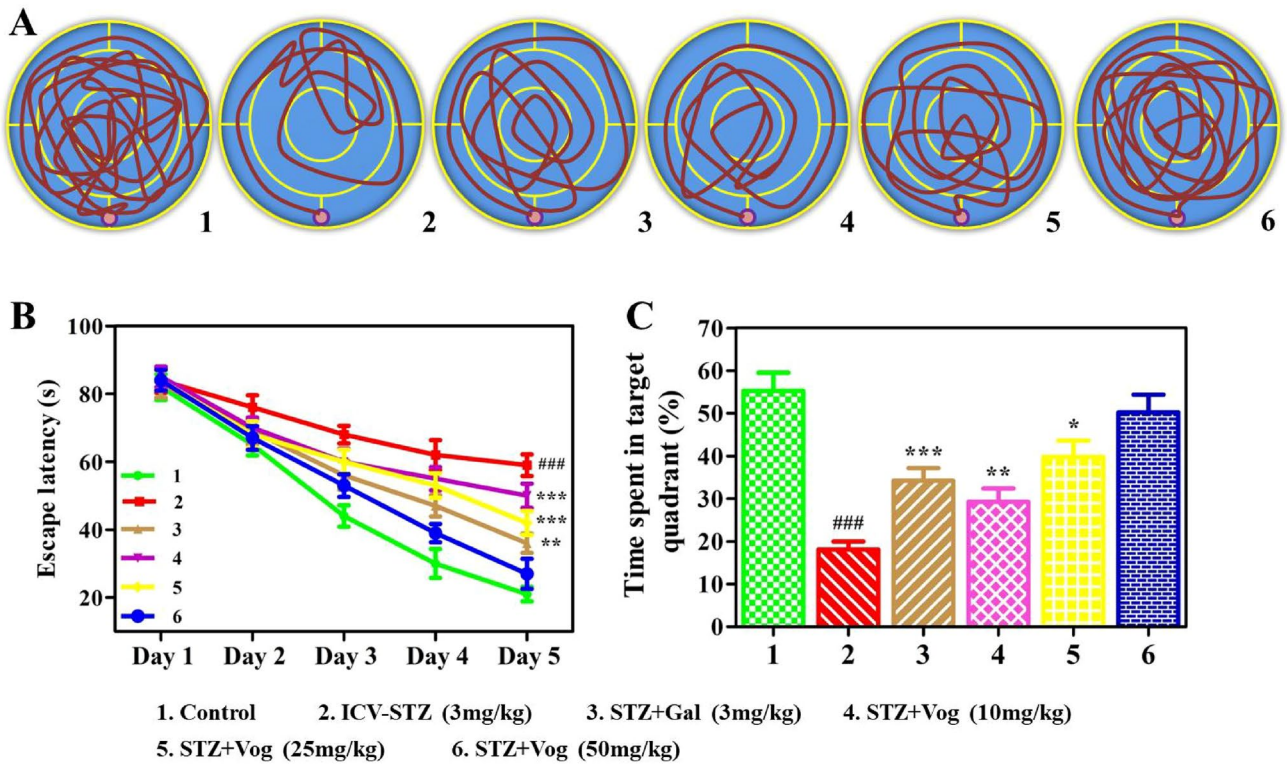

Fig. 2 Effect of Voglibose (10, 25, and 50 mg/kg) treatment in the MWM test on schematic diagram (**A**), escape latency (**B**), and time spent in the target quadrant (**C**) in the probe trial in ICV-STZ-administered rats ($n = 6$). Acquisition data were expressed as a line chart and bar graph (mean ± SD) and analyzed by a two-way ANOVA followed by Bonferroni's post hoc test for multiple comparisons. $^{\#\#}p < 0.01$ and $^{\#\#\#}p < 0.001$ compared to the control group; $^{*}p < 0.05$, $^{**}p < 0.01$, and $^{***}p < 0.0001$ compared to the ICV-STZ group. *ICV-STZ* intracerebroventricular-streptozotocin, *Gal* Galantamine, *Vog* Voglibose

with control group. Treatment with Vog (10, 25, and 50 mg/kg) significantly improved ($p < 0.0001$) TSTQ in comparison to the ICV-STZ-treated group.

Effect of Vog on passive avoidance test

Initial transfer latency (ITL) did not differ significantly among the groups on day 0 (before the STZ treatment). However, following ICV-STZ treatment, a significant attenuation [($F_{(5,20)} = 113.3$, $R^2 = 0.9511$ ($p < 0.0156$)] in step-through latency (STL) was observed in the ICV-STZ-treated group in comparison to the control group. Conversely, treatment with Gal (3 mg/kg) and Voglibose (10, 25, and 50 mg/kg) resulted in a significant improvement of STL in comparison to the ICV-STZ-treated group, which showed a substantial improvement in learning and memory functions. Notably, the administration of the effective dose of Voglibose (50 mg/kg) resulted in a significantly greater improvement of the STL protective effect when compared to the ICV-STZ and Gal-treated groups of rats.

Effect of Vog on Y-maze test

The initial transfer latency (ITL) did not show any significant changes in the groups based on day 0 (before STZ injection). The ICV-STZ-treated rats exhibited a significant improvement [($F_{(5,18)} = 104.2$, $R^2 = 0.9558$ ($p < 0.0073$)] in spontaneous alternation (SA) as compared with control group. Treatment with Gal (3 mg/kg) and Voglibose (10, 25, and 50 mg/kg) significantly attenuate the number of arm entries in the target quadrant, in contrast to ICV-STZ-treated rats. Furthermore, the effective dose treatment with Voglibose (50 mg/kg) significantly attenuated SA and the number of arm entries in the target quadrant as compared to the Gal (3 mg/kg) and ICV-STZ-treated group of rats.

Biochemical measurement

Effect of Vog on AChE activity

The AChE activity was significantly improved in the CS and HS of ICV-STZ rats in the treated group as compared with control group. The administration of Gal (3 mg/kg) and Voglibose (10, 25, and 50 mg/kg) significantly attenuated AChE activity in both brain regions of the CS [($F_{(5,30)} = 237.8$, $R^2 = 0.9754$ ($p < 0.0001$)] and HS [($F_{(5,30)} = 273.6$, $R^2 = 0.9785$ ($p < 0.0001$)] when compared to the ICV-STZ-treated rats. However, Voglibose at a dose of 50 mg/kg demonstrated highly controlled AChE activity compared to Gal and the ICV-STZ treatment group of rats, as shown in Fig. 3A.

Effect of Vog on superoxide dismutase (SOD) activity

In the CS and HS regions, a significant attenuation ($p < 0.001$) was observed in SOD activity in the CS and HS in the ICV-STZ group compared with control group (Fig. 3B). Treatment with Gal (3 mg/kg) and Voglibose (10, 25, and 50 mg/kg) resulted in a significant improvement in both brain regions of the CS [($F_{(5,30)} = 140.8$, $R^2 = 0.9591$ ($p < 0.0001$)] and HS [($F_{(5,30)} = 156.0$, $R^2 = 0.9630$ ($p < 0.0001$)] compared to rats treated with ICV-STZ. In addition, Voglibose at a dose of 50 mg/kg demonstrated highly improved SOD activity when compared to Gal and the ICV-STZ treatment group.

Effect of Vog on catalase (CAT) activity

The ICV injection of STZ significantly attenuated ($p < 0.001$) CAT activity in the CS and HS as compared with control group (Fig. 3C). Treatment with Gal (3 mg/kg) and Voglibose (10, 25, and 50 mg/ml) significantly enhanced CAT activity in the CS [($F_{(5,30)} = 111.2$, $R^2 = 0.9488$ ($p < 0.0001$)] and HS [($F_{(5,30)} = 147.8$, $R^2 = 0.9610$ ($p < 0.0001$)] compared to the ICV-STZ-treated group. Also, the Vog (50 mg/kg)-treated group showed increased CAT antioxidant activity in both the CS and HS regions of experimental rats.

Effect of Vog on GSH activity

The ICV-STZ-treated group significantly attenuated ($p < 0.001$) GSH activity in the CS and HS ($p < 0.001$) when compared with control group (Fig. 3 D). GSH activity was significantly improved in the CS [($F_{(5,30)} = 127.6$, $R^2 = 0.9551$ ($p < 0.0001$)] and HS [($F_{(5,30)} = 209.5$, $R^2 = 0.9722$ ($p < 0.0001$)] in comparison to the ICV-STZ-treated group. Further, Gal (3 mg/kg) and Vog (50 mg/kg) treatment effectively improved the GSH activity in the CS and HS when compared to the ICV-STZ-treated group, and no significant change was observed when compared to the ICV-STZ-treated group of rats.

Effect of Vog on MDA activity

Administration of ICV-STZ-treated groups significantly increased ($p < 0.001$) the MDA activity observed in the CS and HS when compared with control group (Table 1). The treatment with Gal (3 mg/kg) and Vog (10, 25, and 50 mg/ml) for MDA activity was attenuated significantly in the CS [($F_{(5,30)} = 23.51$, $R^2 = 0.9267$ ($p < 0.0001$)] and HS [($F_{(5,30)} = 30.63$, $R^2 = 0.9362$ ($p < 0.0001$)] when compared to the ICV-STZ-treated group. In the group treated with Vog (50 mg/kg), the MDA level was highly controlled, and no significant changes were observed when compared to the ICV-STZ-treated group of rats.

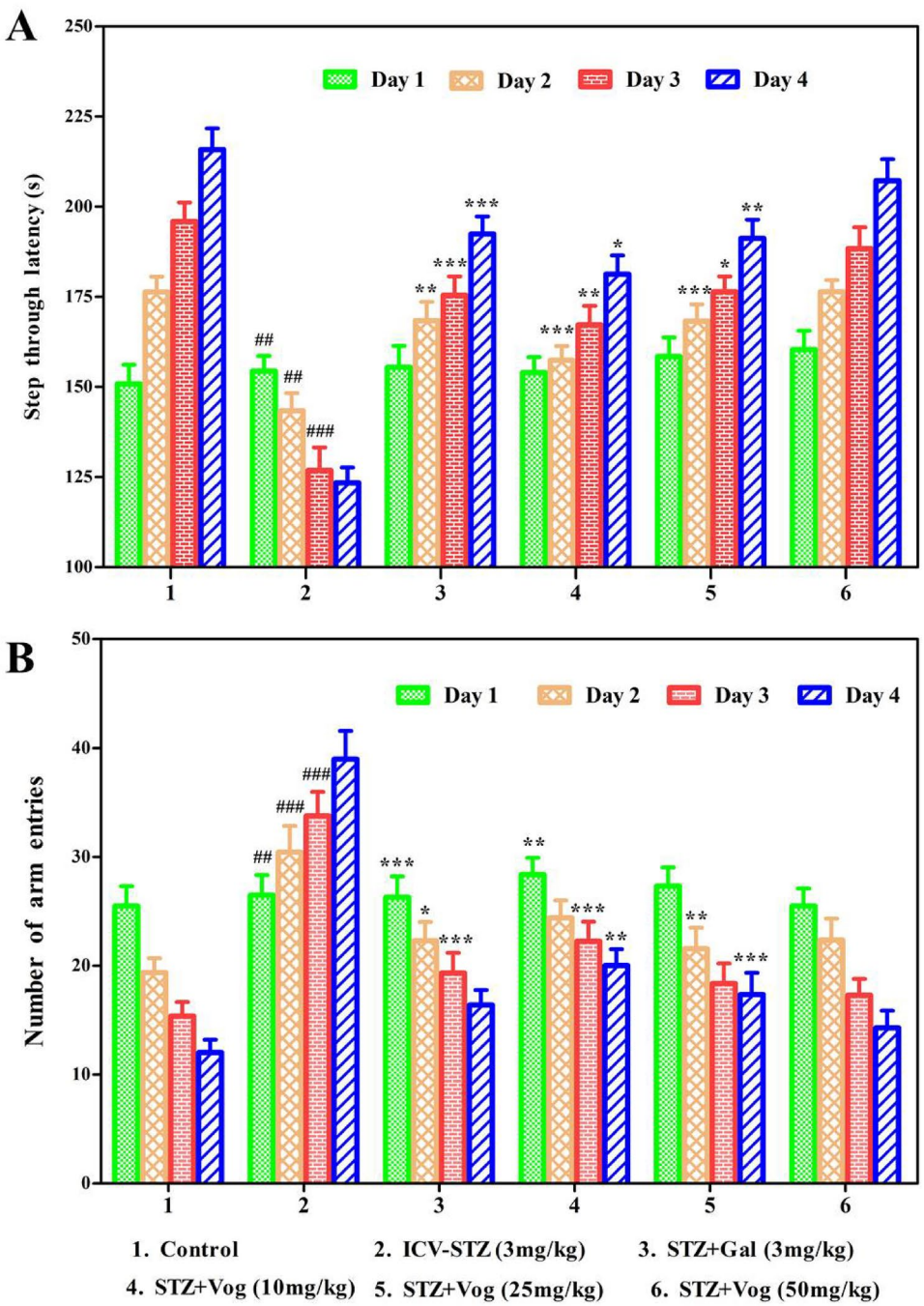

Fig. 3 Effect of Voglibose (10, 25, and 50 mg/kg) treatment in the passive avoidance test (**A**) and Y-maze test (**B**) in ICV-STZ-administered rats ($n=6$). Acquisition data were expressed as a bar graph (mean ± SD) and analyzed by a two-way ANOVA followed by Bonferroni's post hoc test for multiple comparisons. $^{\#\#}p<0.01$ and $^{\#\#\#}p<0.001$ compared to the control group; $^{*}p<0.05$, $^{**}p<0.01$, and $^{***}p<0.0001$ compared to the ICV-STZ group. *ICV-STZ* intracerebroventricular-streptozotocin, *Gal* Galantamine, *Vog* Voglibose

Effect of Vog on nitrite activity

The nitrite activity was significantly improved ($p<0.001$) in the CS and HS in the ICV-STZ-treated group when compared with control group (Table 2). The nitrite activity was significantly attenuated in the treated group with Gal (3 mg/ml) and Vog (10, 25, and 50 mg/ml) in the regions of the CS [($F_{(5,30)}=65.74$, $R^2=0.9810$ ($p<0.0001$)] and HS [($F_{(5,30)}=70.49$, $R^2=0.9816$ ($p<0.0001$)] when compared to the ICV-STZ-treated group. Furthermore, the group treatment with Vog (50 mg/kg) highly controlled the nitrite activity, and no significant changes were observed in the nitrite level when compared to the ICV-STZ-treated group of rats.

Effect of Vog on GPx activity

Administration of ICV-STZ-treated groups significantly attenuated ($p<0.001$) the actuality of GPx in the regions of the CS and HS in the ICV-STZ-treated group when

Table 1 Effect of ICV-STZ-induced AD rats and Voglibose (10, 25 and 50 mg/kg) treatment on oxidative stress markers in different brain regions (cortex and hippocampus)

Treatment group	Brain region	MDA (nM/mg protein)	Nitrite (nM/mg protein)	GPx (nM/mg protein)
Control	Cortex	1.57 ± 0.19	23.93 ± 1.18	152.3 ± 6.38
	Hippocampus	2.67 ± 0.87	34.19 ± 1.57	176.4 ± 6.94
ICV-STZ (3 mg/kg)	Cortex	5.47 ± 0.95$^{###}$	64.28 ± 2.10$^{###}$	75.46 ± 3.72$^{##}$
	Hippocampus	6.89 ± 0.93$^{##}$	88.46 ± 2.76$^{###}$	92.37 ± 4.78$^{##}$
STZ + Gal (3 mg/kg)	Cortex	2.56 ± 0.69***	37.42 ± 1.89*	116.9 ± 5.79***
	Hippocampus	3.50 ± 0.48*	56.28 ± 1.67***	146.8 ± 5.33**
STZ + Vog (10 mg/kg)	Cortex	3.25 ± 0.75**	45.30 ± 1.12**	107.4 ± 4.49*
	Hippocampus	4.94 ± 0.83***	63.39 ± 1.98***	129.5 ± 4.98*
STZ + Vog (25 mg/kg)	Cortex	2.78 ± 0.49***	32.56 ± 0.98*	131.9 ± 4.38***
	Hippocampus	3.41 ± 0.48***	49.28 ± 1.20***	153.59 ± 6.34***
STZ + Vog (50 mg/kg)	Cortex	2.19 ± 0.75	27.60 ± 0.47	145.99 ± 5.89
	Hippocampus	2.93 ± 0.47	38.47 ± 1.22	168.57 ± 6.90

The analysis of data was done by one-way ANOVA followed by Tukey's post hoc test for multiple comparisons. All the values were shown as mean ± SD. $^{##}p < 0.001$, $^{###}p < 0.0001$ compared with control group and $^{*}p < 0.05$, $^{**}p < 0.001$, $^{***}p < 0.0001$ compared with ICV-STZ-treated group

Table 2 Effect of ICV-STZ-induced AD rats and Vog (10, 25, and 50 mg/kg) treatment on mitochondrial respiratory enzyme complexes in different brain regions (cortex and hippocampus)

Treatment group	Brain region	Mitochondrial complex I activity (nM of NADH oxidized/min/ mg protein)	Mitochondrial complex II activity (nM of substrate/min/ mg protein)	Mitochondrial complex III activity (No. of viable cell (% of control)	Mitochondrial complex IV activity (nM cyt-C oxidized/min/ mg protein)
Control	Cortex	92.57 ± 4.25	163.8 ± 6.39	126.8 ± 4.28	106.5 ± 4.75
	Hippocampus	112.8 ± 5.34	187.4 ± 6.90	138.9 ± 6.12	118.9 ± 4.26
ICV-STZ (3 mg/kg)	Cortex	39.78 ± 3.11$^{##}$	75.90 ± 4.22$^{###}$	68.33 ± 3.90$^{##}$	54.37 ± 3.89$^{###}$
	Hippocampus	52.4 ± 3.94$^{###}$	96.78 ± 4.83$^{###}$	74.28 ± 4.39$^{###}$	63.88 ± 4.97$^{##}$
STZ + Gal (3 mg/kg)	Cortex	68.90 ± 3.22**	137.5 ± 5.38*	105.8 ± 4.12**	92.56 ± 3.89*
	Hippocampus	89.4 ± 4.89***	145.6 ± 5.77**	112.3 ± 5.39***	96.80 ± 3.67***
STZ + Vog (10 mg/kg)	Cortex	56.8 ± 2.90*	121.8 ± 4.45**	89.39 ± 4.98*	70.55 ± 4.23***
	Hippocampus	75.87 ± 3.56**	154.7 ± 6.34***	96.99 ± 5.23*	84.36 ± 3.79**
STZ + Vog (25 mg/kg)	Cortex	70.12 ± 3.89***	145.4 ± 5.89**	108.3 ± 4.59***	95.56 ± 4.78***
	Hippocampus	97.65 ± 5.03***	168.6 ± 6.78***	112.9 ± 5.87***	99.89 ± 5.23**
STZ + Vog (50 mg/kg)	Cortex hippocampus	84.57 ± 4.90 104.8 ± 5.88	158.4 ± 6.12 176.1 ± 6.89	119.6 ± 5.22 127.4 ± 5.90	101.8 ± 5.62 113.8 ± 5.89

The analysis of data was done by one-way ANOVA followed by Tukey's post hoc test for multiple comparisons. All the values were shown as mean ± SD. $^{##}p < 0.001$, $^{###}p < 0.0001$ compared with control group and $^{*}p < 0.05$, $^{**}p < 0.001$, $^{***}p < 0.0001$ compared with ICV-STC-treated group

compared with control group (Table 2). The GPx activity was significantly improved in the treated group with Gal (3 mg/kg) and Vog (10, 25, and 50 mg/kg) of the CS [($F_{(5,30)} = 177.5$, $R^2 = 0.9673$ ($p < 0.0001$)] and the HS [($F_{(5,30)} = 157.1$, $R^2 = 0.9632$ ($p < 0.0001$)] when compared to the ICV-STZ-treated group. The group treated with Vog (50 mg/kg) had a highly improved GPx activity, and no significant change was observed in the GPx activity when compared to the ICV-STZ-treated group of rats.

Effect of Vog on mitochondrial complexes (I, II, III, and IV) activity

The activities of four mitochondrial complexes (complex I, II, III, and IV) in the CS and HS regions of ICV-STZ-treated rats were significantly attenuated ($p < 0.001$) when compared with control group.

The mitochondrial complex I activity in CS [($F_{(5,30)} = 123.1$, $R^2 = 0.9535$ ($p < 0.0001$)] and HS [($F_{(5,30)} = 150.6$, $R^2 = 0.9617$ ($p < 0.0001$)] and

mitochondrial complex II activity in CS [($F_{(5,30)} = 156.1$, $R^2 = 0.9630$ ($p < 0.0001$)] and HS [($F_{(5,30)} = 206.5$, $R^2 = 0.9718$ ($p < 0.0001$)] were significantly improved by the treatment with Gal (3 mg/kg) and Vog (10, 25, and 50 mg/kg) in the CS and HS regions (Table 2). All the reversals by the treatment were in comparison to the ICV-STZ group. The Vog (50 mg/kg) group treatment in both regions of the CS and HS was highly improved and did not show a significant difference in complex I and complex II activities.

Treatment with Gal (3 mg/kg) and Vog (10, 25, and 50 mg/kg) significantly improved in the mitochondrial complex III activity in CS [($F_{(5,30)} = 102.5$, $R^2 = 0.9447$ ($p < 0.0001$)] and HS [($F_{(5,30)} = 131.9$, $R^2 = 0.9565$ ($p < 0.0001$)] and mitochondrial complex IV activity in CS [($F_{(5,30)} = 109.8$, $R^2 = 0.9482$ ($p < 0.0001$)] and HS [($F_{(5,30)} = 117.3$, $R^2 = 0.9513$ ($p < 0.0001$)] as compared to the ICV-STZ group (Table 2). Furthermore, the treatment with Vog (50 mg/kg) showed highly improved complex III and IV activity in both the CS and HS as compared to the ICV-STZ group (Fig. 4).

Effect of Vog on neuroinflammation activity

TNF-α, IL-6, and CRP were evaluated in the HS, and results indicated significantly improved levels of the above three neuroinflammation markers in the ICV-STZ group [($F_{(5,30)} = 325.0$, $R^2 = 0.9887$ ($p < 0.0001$)] compared with control group. However, the TNF-α level was significantly decreased with the treatments with Gal (3 mg/kg) and Vog (10, 25, and 50 mg/kg) as compared to the ICV-STZ group (Fig. 5 A). The group treatment with Gal (3 mg/kg) and Vog (10, 25, and 50 mg/kg) significantly attenuated [($F_{(5,30)} = 65.83$, $R^2 = 0.9269$ ($p < 0.0001$)] IL-6 levels when compared to the ICV-STZ-treated group of rats (Fig. 5B). The treated group with Gal (3 mg/kg) and Vog (10, 25, and 50 mg/kg) produced significant attenuation [($F_{(5,30)} = 84.76$, $R^2 = 0.9339$ ($p < 0.0001$)] in terms of CRP level in the HS as compared to ICV-STZ-induced rats (Fig. 5C).

Western blot analysis

The protective effect of Gal (3 mg/kg) and Vog (10, 25, and 50 mg/kg) against ICV-STZ-induced Aβ aggregation was analyzed with the help of protein markers. As expected, Aβ protein was increased in the CS and HS regions of the ICV-STZ-treated group compared with control group (Fig. 6A and B). Interestingly, treatment with Vog (50 mg/kg) group regions of both CS and HS results showed a significantly attenuated ($p < 0.001$) expression of Aβ aggregation compared with the Gal (3 mg/kg) and ICV-STZ-treated group. This result suggests that the neuroprotective function of Vog on ICV-STZ-induced Aβ aggregation may occur by controlling the Aβ protein.

Histopathological analysis

The findings from histopathological changes observed in the brain parts of the CS and HS (CA1, CA3, and DG) treated with different experimental groups are shown in Fig. 7. The histology photographs of the CS and HS parts showed tissues and neuronal cells with similar damage in the ICV-STZ-treated group when compared with control group. Specifically, a histopathological examination found that the Gal (3 mg/kg) and Vog (10, 25, and 50 mg/kg) treated groups were examined to observe the CS and HS (CA1, CA3, and DG) parts for decreased neuronal damage, healthy neuron cells with clear cytoplasm, and healthy tissues when compared to the ICV-STZ-treated group of rats (Fig. 7). In addition, minimal focal necrosis and cell damage in the major vital organs, such as the heart, kidney, liver, and histiocytosis in the lungs were observed in the treatment with ICV-STZ group as compared with control group. The treatment with Gal (3 mg/kg) and Vog (10, 25, and 50 mg/kg) groups showed highly improved vital organs when compared with the ICV-STZ-treated group (Fig. 8). Based on the results of the current study, Vog (50 mg/kg) is highly improved in tissues and cells, and adverse effects were observed in experimental rats.

Discussion

Alzheimer's disease is often associated with a decline in cognitive function through degeneration of cholinergic neurons in the brain, Aβ aggregation, and impairment of central insulin signaling (Ma et al. 2021; Gallego Villarejo et al. 2022). Several experimental lines of evidence suggest that autopsies of AD patients demonstrate decreased insulin receptor expression and downstream signaling in the brain. By reducing Aβ aggregation, AChE levels and increasing mitochondrial complex activity by increasing antioxidant activity, AD can be controlled (Akhtar et al. 2020a, b; Salkovic-Petrisic et al. 2013). However, to the best of our knowledge, no one has yet investigated the pivotal study of reducing Aβ aggregation, AChE, and neuroinflammation levels using the drug Voglibose in central insulin resistance of ICV-STZ-induced AD. Therefore, the present study aimed to investigate the additional neuroprotective effect of Voglibose in rat models of ICV-STZ-induced neuronal damages, mitochondrial dysfunction, neuroinflammation, histopathological changes, and cholinergic functions. Therefore, we evaluated the effect of Voglibose with the standard drug of Galantamine.

The injection of ICV-STZ is a method that induces brain insulin resistance and replicates pathological and behavioral

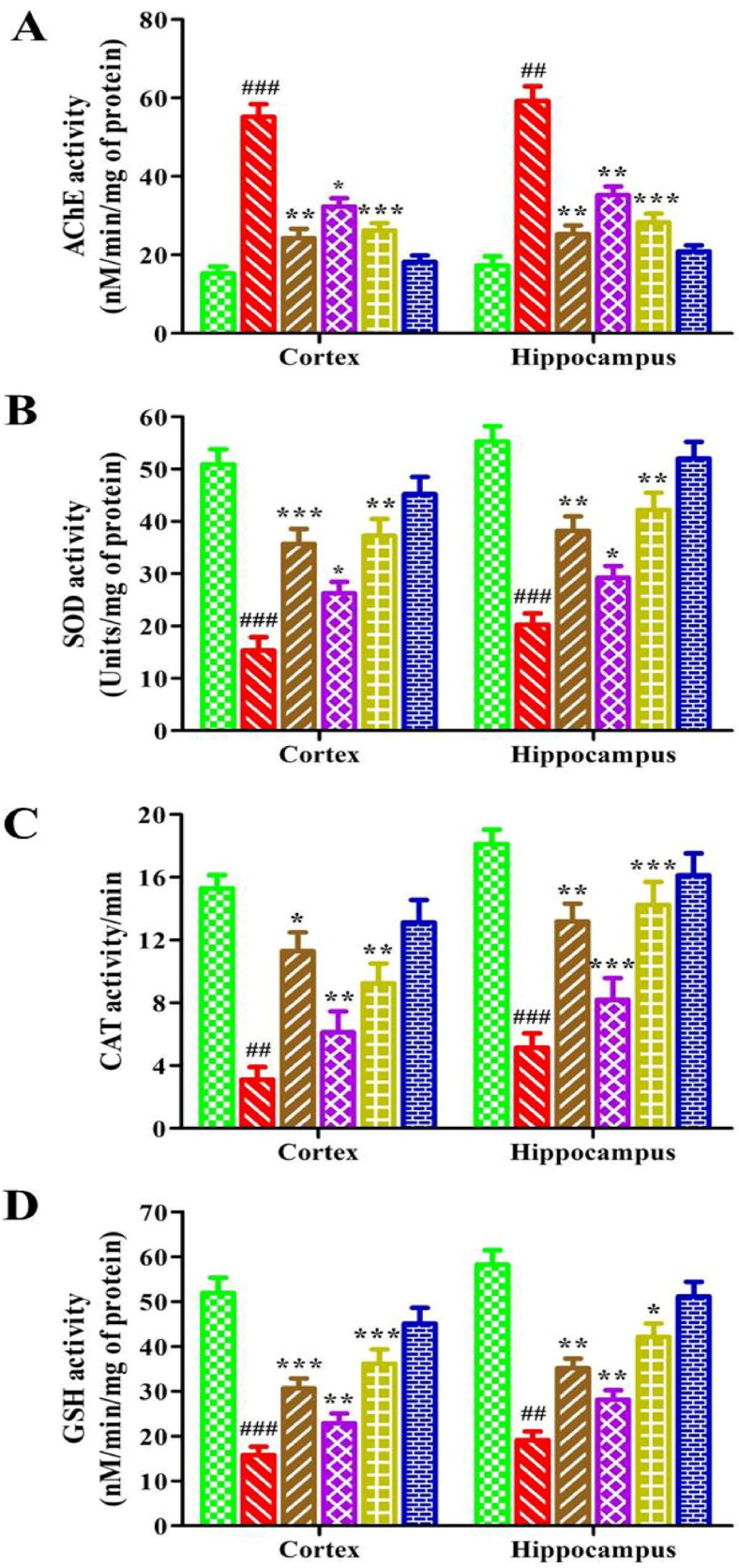

Fig. 4 Effect of Voglibose (10, 25, and 50 mg/kg) treatment on AChE activity (**A**), SOD activity (**B**), CAT activity (**C**), and GSH activity (**D**) in ICV-STZ-administered rats. Acquisition data were expressed as a bar graph (mean ± SD) and analyzed by one-way ANOVA followed by Tukey's post hoc test for multiple comparisons. $^{\#\#}p < 0.01$ and $^{\#\#\#}p < 0.001$ compared to the control group; $^{*}p < 0.05$, $^{**}p < 0.01$, and $^{***}p < 0.0001$ compared to the ICV-STZ group. *ICV-STZ* intracerebroventricular-streptozotocin, *Gal* Galantamine, *Vog* Voglibose

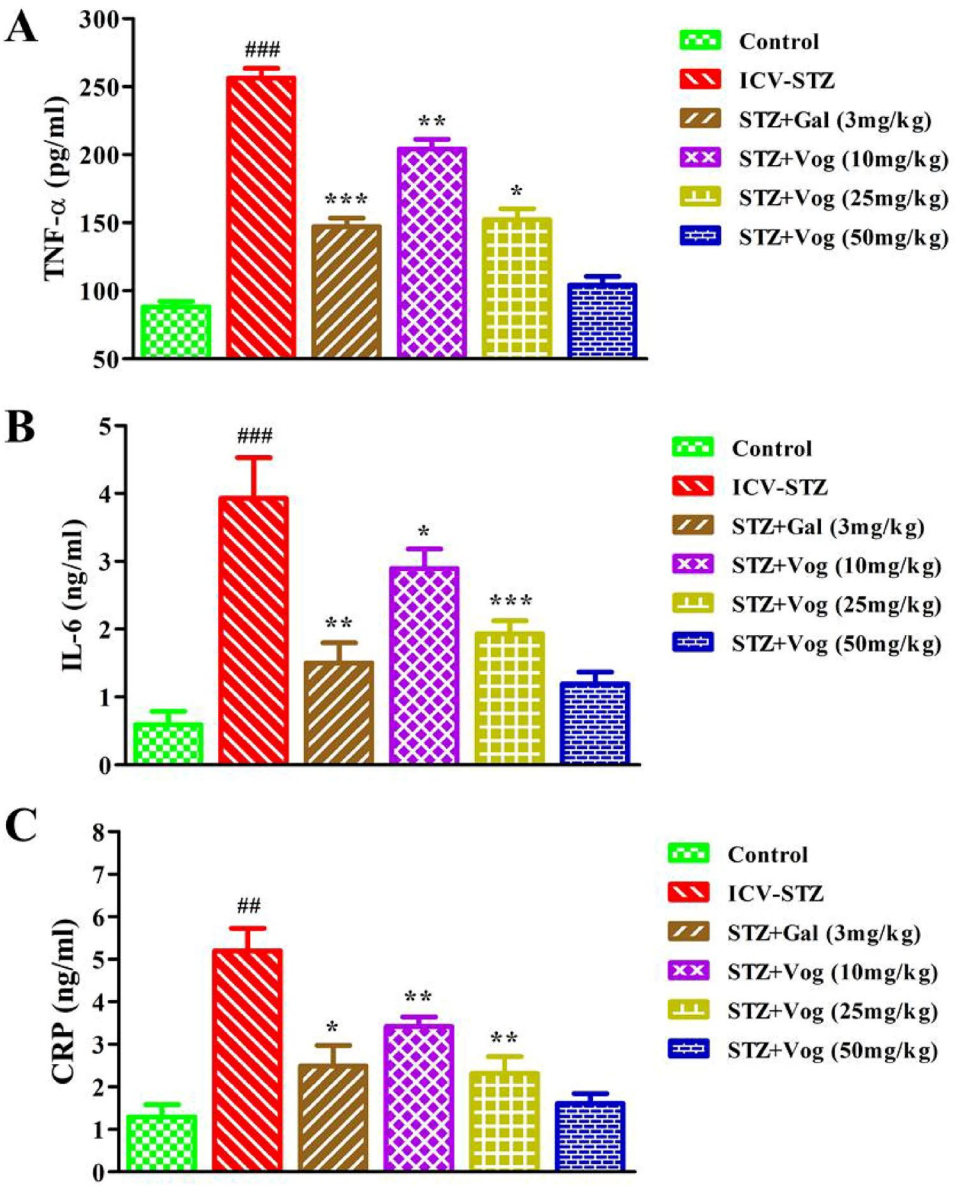

Fig. 5 Effect of Gal and Voglibose on a TNF-α (**A**), IL-6 (**B**), and CRP (**C**). Acquisition data were expressed as a bar graph (mean ± SD) and analyzed by one-way ANOVA followed by Tukey's post hoc test for multiple comparisons. $^{\#\#}p < 0.01$ and $^{\#\#\#}p < 0.001$ compared to the control group; $^{*}p < 0.05$, $^{**}p < 0.01$, and $^{***}p < 0.0001$ compared to the ICV-STZ group. *ICV-STZ* intracerebroventricular-streptozotocin, *Gal* Galantamine, *Vog* Voglibose

changes that occur in AD, such as cognitive dysfunction, mitochondrial dysfunction, and oxidative stress (Sachdeva et al. 2014; Agrawal et al. 2020). Administering a sub-diabetogenic dose of ICV-STZ results in oxidative stress, the release of inflammatory cytokines, mitochondrial dysfunction, and impaired insulin signaling. Consequently, the CS and HS regions of the brain experience insulin signaling disruption, initiating neurodegenerative processes that eventually lead to cognitive dysfunction (Mishra et al. 2018; Akhtar et al. 2020a, b). However, limitations to this model exist since, although administering ICV-STZ to rats produces neuropathological and behavioral symptoms that simulate AD, a complete resemblance to AD is not evident, and clear explanations for these phenomena are yet to be established (Wang et al. 2012a, b; Kim et al. 2019). The ICV-STZ model showed that the primary indicator of behavioral abnormalities involves cognitive dysfunction. Our research uncovered that the injection of STZ resulted in memory impairment, which we evaluated using the MWM and PA tests. Moreover, the increasing mean escape latency and swim path length, coupled with reduced TSTQ confirmed the impaired retention memory in ICV-STZ rats during the spatial navigation task in MWM. The administration of Voglibose treatment improved the retention memory of ICV-STZ animals by considerably decreasing the mean escape latency, enabling them to find the hidden platform sooner, and spending more time in the target quadrant compared to their counterparts. The findings of this study are consistent with previous studies showing that treatment with vitamin D3 improves spatial learning and memory function in MWM (Yamini et al.

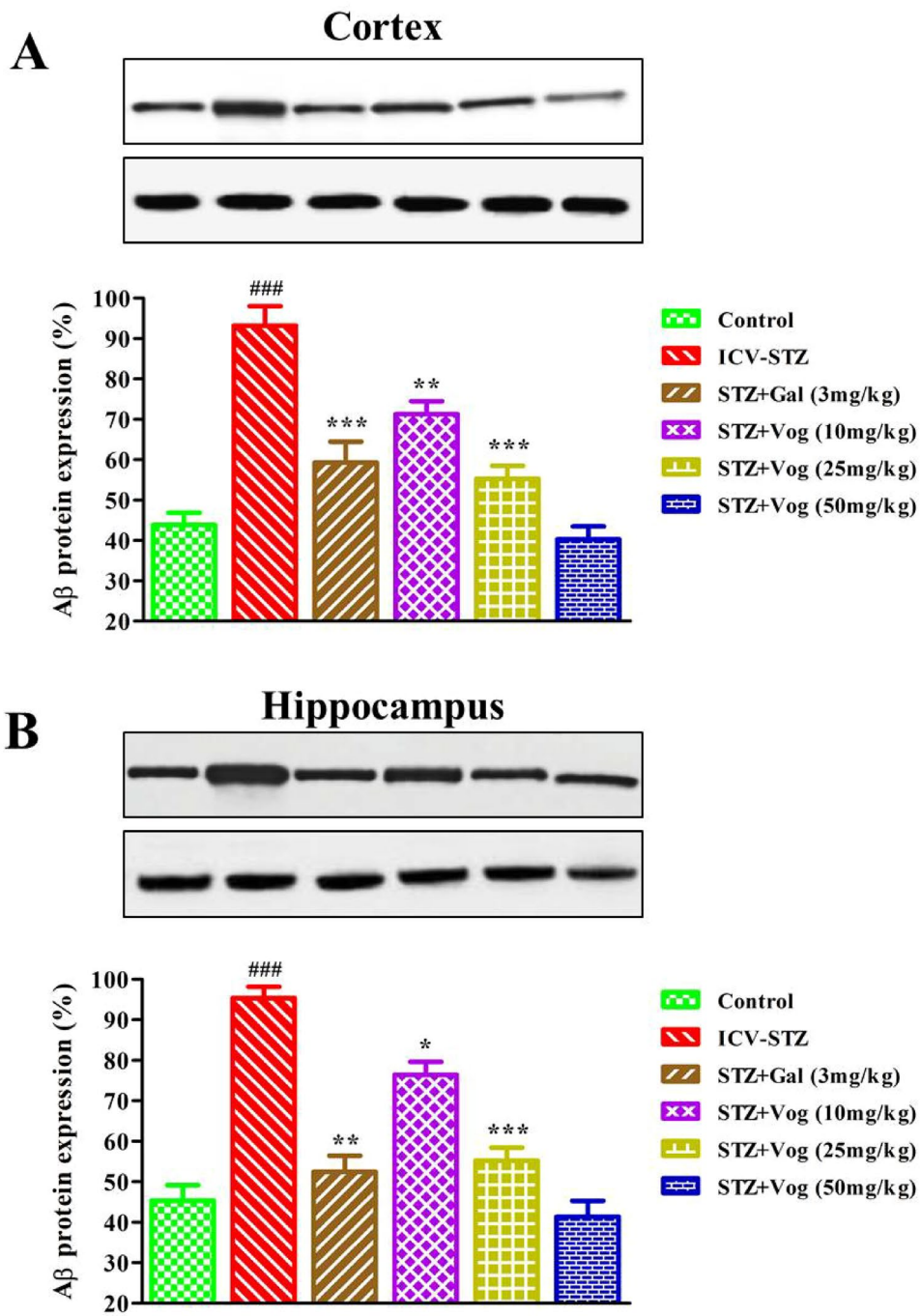

Fig. 6 Western blot analysis of Aβ protein expression shows that it is downregulated in the cortex and hippocampus of the ICV-STZ-treated rats and reversed by Gal (3 mg/kg) and Vog (10,25, and 50 mg/kg). β-Actin was used as a loading control (**A**). Quantification of Aβ protein expression was analyzed as the ratio (%) in the cortex and hippocampus regions. Acquisition data were expressed as a bar graph (mean ± SD) and analyzed by one-way ANOVA followed by Tukey's post hoc test for multiple comparisons. ###$p < 0.001$ compared to the control group; **$p < 0.01$, and ***$p < 0.0001$ compared to the ICV-STZ group. *ICV-STZ* intracerebroventricular-streptozotocin, *Gal* Galantamine, *Vog* Voglibose

2018). Additionally, Voglibose treatment demonstrated an improvement in retention memory function by increasing the transfer latency into the dark compartment, as evidenced in STL by the PA test. Voglibose-treated animals exhibited improved retention memory compared to ICV-STZ animals in the Y-maze task and decreased the number of arm entries into the open-arm entries. Although Voglibose treatment strategies elicited improved spatial learning, they also demonstrated prominent superior efficacy in attenuating ICV-STZ-induced neuronal damage and behavioral dysfunction.

Previous studies suggest that the cholinergic system in the brain, which is vital for learning and memory, may be closely linked to age-related diseases such as AD. Choline acetyltransferase (ChAT) is a specific protein marker of cholinergic neurons, playing a crucial role in maintaining acetylcholine (ACh) levels (Cheung et al. 2012; Cheung et al. 2012). Its synthesis requires acetyl CoA, which results from the breakdown of glucose and insulin and is regulated by insulin (Zhang et al. 2007). Our study indicates that ICV-STZ induces a notable

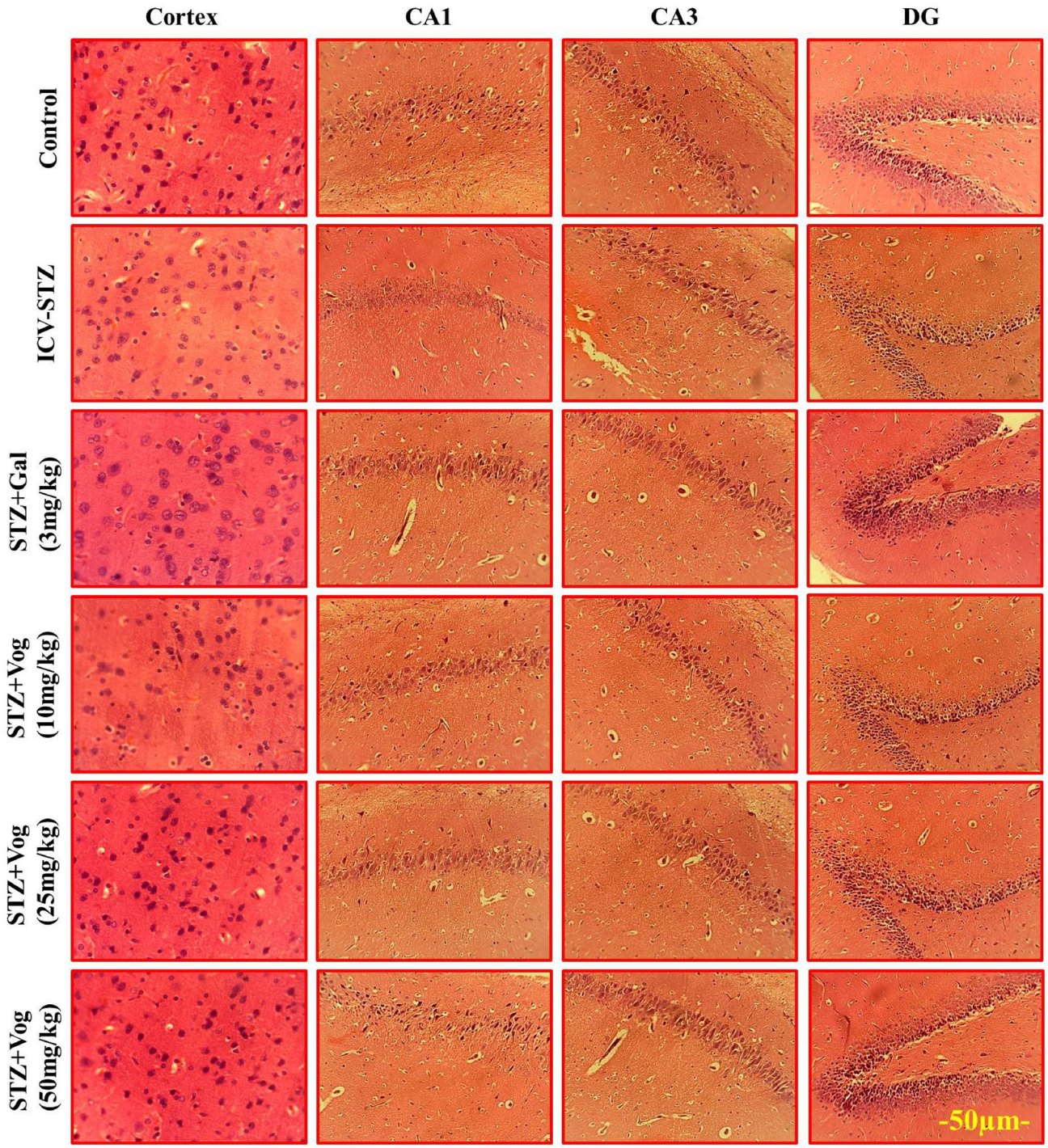

Fig. 7 Effects of Gal and Voglibose treatment on histological changes of ICV-STZ-induced neuronal damage in the cortex and hippocampal CA1, CA3, and DG regions. Scale bar: 50 µm. *ICV-STZ* intracerebroventricular-streptozotocin, *Gal* Galantamine, *Vog* Voglibose

increase in AChE activity, which was regulated through the administration of different doses of Voglibose (10, 25, and 50 mg/kg). The ICV-STZ is known to induce persistent cognitive impairments related to reduced activity of choline acetyltransferase (ChAT) and AChE. This study describes that the ameliorating effects of Voglibose against ICV-STZ-induced AChE activity may be attributed to its antioxidant actions, as the increase in reactive oxygen species (ROS) and lipid peroxidation has been shown to enhance AChE activity.

The brain is one of the most metabolically active organs and has a limited number of endogenous defense systems,

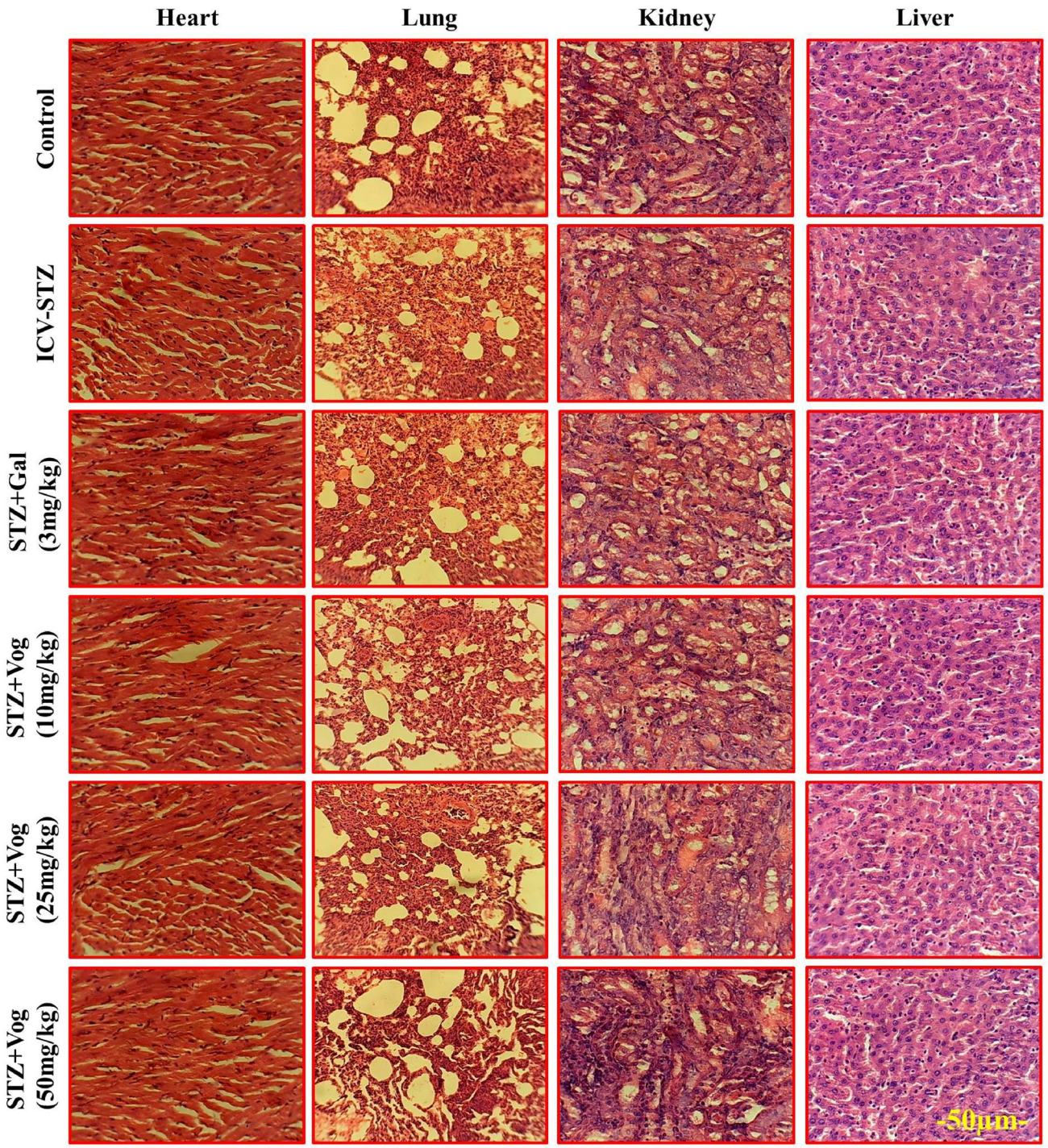

Fig. 8 Effects of Gal and Voglibose treatment on histological changes in major vital organs such as the heart, lung, kidney, and liver in the experimental animals. Scale bar: 50 μm. *ICV-STZ* intracerebroventricular-streptozotocin, *Gal* Galantamine, *Vog* Voglibose

thus making it highly susceptible to oxidative tissue damage caused by free radicals (Salkovic-Petrisic et al. 2013). Protection against brain oxidative stress comes from endogenous antioxidant enzymes such as GSH, SOD, CAT, and GPx (Sharma et al. 2012). Neuronal oxidative stress, triggered by ICV-STZ, causes damage to cellular biomolecules, including proteins, DNA, RNA, and lipids, and is a key factor in the progression of neurodegenerative disorders like AD (Lu et al. 2017; Leyane et al. 2022). Our study discovered that Voglibose treatment, at doses of 10, 25, and 50 mg/kg,

significantly reduced ICV-STZ-induced oxidative stress and restored the endogenous antioxidant defense system nearly to basal levels. Moreover, treatment with Voglibose (50 mg/kg) restored all antioxidant activities, confirming the restoration of the depleted endogenous antioxidant defense system and demonstrating Voglibose's potential as an antioxidant to reduce oxidative damage, consistent with previous reports (Sharma et al. 2012).

Increased neuronal oxidative stress worsens peroxidative damage of membrane lipids through MDA generation and nitric oxide production, which in turn amplifies neuronal damage severely affecting key cellular biomolecules and is commonly used as biomarkers of oxidative damage (Leyane et al. 2022; Singh et al. 2023). In the present study, ICV-STZ-induced overproduction of free radicals triggered MDA, and nitric oxide-mediated hippocampal and CS parts showed oxidative damage. Our results revealed decreased levels of MDA and nitrite for protein carbonylation after treatment with Voglibose. This suggests and confirms the oxidative stress-neutralizing capacity and protective effect of Voglibose against ICV-STZ-treated rats. Our findings are consistent with previous experimental evidence that antioxidant activity restores and decreases oxidative damage (Yamini et al. 2018).

Neuronal mitochondrial dysfunction may be both a cause and consequence of ROS generation. ICV-STZ treatment significantly increased plasma nitric oxide levels, leading to oxidative-nutritive damage and confirming that it induces peroxynitrite-mediated neuronal damage and apoptosis by affecting mitochondrial complex functions (I, II, III, and IV) (Tirichen et al. 2021; Cheng et al. 2020). However, Voglibose treatment effectively reduced ICV-STZ-induced oxidative-nitrite damage and restored mitochondrial complex activities, thus confirming the potential neuroprotective effect of Voglibose. This demonstrates that Voglibose antioxidant properties are crucial in mitigating ICV-STZ-induced mitochondrial aberrations, neurotoxicity, and cognitive impairment. Interestingly, these findings are consistent with a study showing that vitamin D can also restore mitochondrial complex functions (Yamini et al. 2018).

In the ICV-STZ model of AD, neuroinflammation plays a significant role in synaptic dysfunction and neurodegeneration. The ICV-STZ causes microglia activation, resulting in the release of pro-inflammatory cytokines TNF-α and IL-6, leading to neuroinflammation. Recent experimental evidence suggests that chronic neuroinflammation conditions can accelerate disease progression in AD pathology (Tezel 2022; Leng et al. 2021). Elevated levels of TNF-α and CRP have been negatively correlated with neurodegenerative diseases like AD, which supports targeting anti-inflammatory mechanisms as a potential method to decrease AD progression (Singhet al. 2023). Vitamin D3 has been found to have anti-inflammatory properties, according to recent experimental evidence (Yamini et al. 2018). Our study showed that Voglibose effectively modulates neuroinflammation by reducing pro-inflammatory cytokine levels, such as TNF-α and IL-6. The mechanism by which Voglibose inhibits the levels of TNF-α, IL-6, and CRP may involve partially attenuating oxidative stress pathways and inhibiting pathways. Voglibose treatment also reduced ICV-STZ-induced inflammatory damage in the HS. This result could be well correlated with increased cell survival and the reversal of neuronal injury.

The amyloidogenic hypothesis has gained widespread acceptance as the leading theory for the development of AD (Sanchez-Rodriguez et al. 2023). This hypothesis posits that the extracellular deposition of Aβ, resulting from the upregulation of APP and increased aggregation of Aβ, is responsible for the neuronal damage that leads to oxidative stress, activation of inflammatory responses, and synaptic dysfunction, eventually culminating in cognitive deficits (Leyane et al. 2022; Xue et al. 2022). By administering ICV-STZ, we observed an increase in the total tau protein and β-amyloid, coupled with changes in the mRNA transcripts and proteins of insulin signaling pathways and AD-related genes (APP and tau protein) in the brain due to a decreased GSK-3alpha/beta ratio (phosphorylated/total) (Andrade et al. 2023). Our study corroborates previous findings on the ICV-STZ model, as we too observed increased gene expression of Aβ aggregation following administration. However, our treatment with Vog (Vog 50 mg/kg) proved to be neuroprotective, as it reduced APP expression and attenuated Aβ accumulation, potentially combating neuroinflammation and oxidative stress. This was achieved by enhancing the cleavage of APP by α-secretase and preventing the deposition of amyloid-β protein.

The histological examination provides for evaluating neuronal changes and drug action. The HS plays a well-established role in learning and memory (Mishra et al. 2018). Previous studies have shown that ICV-STZ can lead to neurodegeneration in the HS, which contributes significantly to AD pathology. According to histopathological evidence, ICV-STZ disrupts both the structural and functional aspects of cortical and hippocampal structures. Additionally, it leads to the formation of β-amyloid peptide-like aggregates in brain capillaries (Karthick et al. 2019). In our study, we observed remarkable morphological changes in the hippocampal CA1, CA3, and DG parts and the CS of ICV-STZ-induced AD animals. However, Voglibose treatment effectively attenuated ICV-STZ-induced morphological alterations in the hippocampal CA1, CA3, DG, and CS regions, leading to functional neurotherapeutic benefits and thereby, improvements in cognitive functions (Arezoumandan et al. 2022). Histopathological analysis showed that the HS of ICV-STZ-treated rats

had a greater number of damaged neurons with shrunken morphology as compared with control group. However, administration of Voglibose significantly protected healthy neurons against ICV-STZ-induced neuronal toxicity and loss, characterized by clear nuclei with an oval shape. Additionally, Voglibose treatment had a much higher ameliorative effect on oxidative biomarkers and enzymatic activities in the heart, liver, kidney, and lung tissues of the experimental group than the ICV-STZ-treated group.

Conclusion

In conclusion, the present study demonstrated that Gal and Voglibose supplementation potentially reverses ICV-STZ-induced alterations in the cognitive behavioral activity of spatial and non-spatial memory functions in the experimental rats. In a nutshell, this study can be concluded that in most of the biochemical and histopathological studies, amyloid-β protein expression in the CS and HS of Gal (3 mg/kg) Voglibose (10, 25, and 50 mg/kg) drug treatment was found to be more effective. Our study discovered that Voglibose treatment significantly reduced ICV-STZ-induced oxidative stress and restored the endogenous antioxidant defense system to nearly basal levels. The neuroprotective effect of Voglibose could be attributed to its possible involvement in modulating neuroinflammation (TNF-α, IL-6, and CPR) brain damage, decreasing neuronal oxidative stress, improving mitochondrial complex activities (I, II, III, and IV), and enhancing cholinergic neurotransmission. It reversed some of the core features of the AD model, such as oxidative stress, neuroinflammation, and mitochondrial dysfunction in the regions of the CS and HS. Moreover, Voglibose controlled ICV-STZ-induced central insulin resistance by targeting the Aβ aggregation neuronal pathways. Furthermore, Voglibose treatment effectively reversed ICV-STZ-induced neuronal damage in hippocampal CA1, CA3, DG, and CS parts of the brain. This ensures that neuronal cells with healthy and clear cytoplasm can be restored. Therefore, our study underscores the functional importance of prophylactic maintenance of adequate Voglibose and might offer a novel therapeutic strategy for the treatment of neurodegenerative diseases such as AD.

Acknowledgements This work was financially supported by University Research Fellow (URF) from Periyar University, Salem 636011, Tamil Nadu, India (PU/AD-3/ URF/ 013805/ 2019).

Funding The authors have not disclosed any funding.

Data availability Data will be made available on request.

Declarations

Conflict of interest The authors declare that there were no conflicts of interest.

References

Agrawal M, Perumal Y, Bansal S, Arora S, Chopra K (2020) Phycocyanin alleviates ICV-STZ induced cognitive and molecular deficits via PI3-Kinase dependent pathway. Food Chem Toxicol 145:111684

Ahn Y, Seo J, Park J, Won J, Yeo HG, Kim K, Jeon CY, Huh JW, Lee SR, Lee DS, Lee Y (2020) Synaptic loss and amyloid-beta alterations in the rodent HS induced by streptozotocin injection into the cisterna magna. Lab Anim Res 36:1–6

Akhtar A, Bishnoi M, Sah SP (2020a) Sodium orthovanadate improves learning and memory in intracerebroventricular-streptozotocin rat model of Alzheimer's disease through modulation of brain insulin resistance induced tau pathology. Brain Res Bull 1(164):83–97

Akhtar A, Dhaliwal J, Saroj P, Uniyal A, Bishnoi M, Sah SP (2020b) Chromium picolinate attenuates cognitive deficit in ICV-STZ rat paradigm of sporadic Alzheimer's-like dementia via targeting neuroinflammatory and IRS-1/PI3K/AKT/GSK-3β pathway. Inflammopharmacol 28:385–400

Arezoumandan S, Xie SX, Cousins KA, Mechanic-Hamilton DJ, Peterson CS, Huang CY, Ohm DT, Ittyerah R, McMillan CT, Wolk DA, Yushkevich P (2022) Regional distribution and maturation of tau pathology among phenotypic variants of Alzheimer's disease. Acta Neuropathol 144(6):1103–1116

Association A (2017) Alzheimer's disease facts and figures. Alzheimers Dement 13(4):325–373

Berman SB, Hastings TG (1999) Dopamine oxidation alters mitochondrial respiration and induces permeability transition in brain mitochondria: implications for Parkinson's disease. J Neurochem 73(3):1127–1137

Cheng H, Gang X, Liu Y, Wang G, Zhao X, Wang G (2020) Mitochondrial dysfunction plays a key role in the development of neurodegenerative diseases in diabetes. Am J Physiol Endocrinol 318(5):E750–E764

Cheung J, Rudolph MJ, Burshteyn F, Cassidy MS, Gary EN, Love J, Franklin MC, Height JJ (2012) Structures of human acetylcholinesterase in complex with pharmacologically important ligands. J Med Chem 55(22):10282–10286

Claiborne AJ (1985) Handbook of methods for oxygen radical research. CRC Press, Boca Raton, pp 283–284

Conrad CD, Galea LA, Kuroda Y, McEwen BS (1996) Chronic stress impairs rat spatial memory on the Y maze, and this effect is blocked by tianeptine treatment. Behav Neurosci 110(6):1321

Derosa G, Maffioli P (2012) Mini-Special Issue paper Management of diabetic patients with hypoglycemic agents α-Glucosidase inhibitors and their use in clinical practice. Arch Med Sci 8 (5): 899–906

Ellman GL, Courtney KD, Andres V Jr, Featherstone RM (1961) A new and rapid colorimetric determination of acetylcholinesterase activity. Biochem Pharmacol 7(2):88–95

Gallego Villarejo L, Bachmann L, Marks D, Brachthauser M, Geidies A, Muller T (2022) Role of intracellular amyloid β as pathway modulator, biomarker, and therapy target. Int J Mol Sci 23(9):4656

Green LC, Wagner DA, Glogowski J, Skipper PL, Wishnok JS, Tannenbaum SR (1982) Analysis of nitrate, nitrite, and [15N] nitrate in biological fluids. Analyt Biochem Anal Biochem 126(1):131–138

Hatai J, Motiei L, Margulies D (2019) Analyzing amyloid beta aggregates with a combinatorial fluorescent molecular sensor. J Amer Chem Soci 139(6):2136–2139

Jayant S, Sharma BM, Bansal R, Sharma B (2016) Pharmacological benefits of selective modulation of cannabinoid receptor type 2 (CB2) in experimental Alzheimer's disease. Pharmacol Biochem Behav 1(40):39–50

Jollow DJ, Mitchell JR, Zampaglione NA, Gillette JR (1974) Bromobenzene-induced liver necrosis. Protective role of glutathione and evidence for 3,4 bromobenzene oxide as the hepatotoxic metabolite. Pharmacol 11(3):151–169

Kareem RT, Abedinifar F, Mahmood EA, Ebadi AG, Rajabi F, Vessally E (2021) The recent development of donepezil structure-based hybrids as potential multifunctional anti-Alzheimer's agents: highlights from 2010 to 2020. RSC Adv 11(49):30781–30797

Karthick C, Nithiyanandan S, Essa MM, Guillemin GJ, Jayachandran SK, Anusuyadevi M (2019) Time-dependent effect of oligomeric amyloid-β (1–42)-induced hippocampal neurodegeneration in rat model of Alzheimer's disease. Neurol Res 41(2):139–150

Kim JW, Lee YJ, You YH, Moon MK, Yoon KH, Ahn YB, Ko SH (2019) Effect of sodium-glucose cotransporter 2 inhibitor, empagliflozin, and α-glucosidase inhibitor, voglibose, on hepatic steatosis in an animal model of type 2 diabetes. J Cell Biochem 120(5):8534–8546

King TE, Howard RL (1976) Preparations and properties of soluble NADH dehydrogenases from cardiac muscle. I Meth Enzym 10:275–294

Kono Y (1978) Generation of superoxide radical during autoxidation of hydroxylamine and an assay for superoxide dismutase. Arch Biochem Biophy 186(1):189–195

Lawrence RA, Burk RF (1976) Glutathione peroxidase activity in selenium-deficient rat liver. Biochem Biophys Res Commun 71(4):952–958

Leng F, Edison P (2021) Neuroinflammation and microglial activation in Alzheimer disease: where do we go from here? Nat Rev Neurol 17(3):157–172

Leyane TS, Jere SW, Houreld NN (2022) Oxidative stress in ageing and chronic degenerative pathologies: molecular mechanisms involved in counteracting oxidative stress and chronic inflammation. Int J Mol Sci 23(13):7273

Lowry OH, Rosebrough NJ, Farr AL, Randall RJ (1951) of these enzymes than MQ. J Biol Chem 193:265–275

Lu Y, Dong Y, Tucker D, Wang R, Ahmed ME, Brann D, Zhang Q (2017) Treadmill exercise exerts neuroprotection and regulates microglial polarization and oxidative stress in a streptozotocin-induced rat model of sporadic Alzheimer's disease. J Alzheimer's Dis 56(4):1469–1484

Ma M, Liu Z, Gao N, Dong K, Pi Z, Kang L, Du X, Ren J, Qu X (2021) Near-infrared target enhanced peripheral clearance of amyloid-β in Alzheimer's disease model. Biomater 1(276):121065

Malik R, Kalra S, Bhatia S, Al Harrasi A, Singh G, Mohan S, Makeen HA, Albratty M, Meraya A, Bahar B, Tambuwala MM (2022) Overview of therapeutic targets in management of dementia. Biomed Pharmacother 1(152):113168

Mishra SK, Singh S, Shukla S, Shukla R (2018) Intracerebroventricular streptozotocin impairs adult neurogenesis and cognitive functions via regulating neuroinflammation and insulin signaling in adult rats. Neurochemistry International Neurochem Int 1(113):56–68

Moritoh Y, Takeuchi K, Hazama M (2010) Combination treatment with alogliptin and voglibose increases active GLP-1 circulation, prevents the development of diabetes and preserves pancreatic beta-cells in prediabetic db/db mice. Diabetes Obes Metab 12(3):224–233

Morris R (1984) Developments of a water-maze procedure for studying spatial learning in the rat. J Neurosci Methods 11(1):47–60

Mosmann T (1983) Rapid colorimetric assay for cellular growth and survival: application to proliferation and cytotoxicity assays. J Immunol Methods 65(1–2):55–63

Paxinos G, Watson CR, Emson PC (1980) AChE-stained horizontal sections of the rat brain in stereotaxic coordinates. J Neurosci Methods 3(2):129–149

Ramagiri S, Taliyan R (2017) Remote limb ischemic post conditioning during early reperfusion alleviates cerebral ischemic reperfusion injury via GSK-3β/CREB/BDNF pathway. Eur J Pharmacol 15(803):84–93

Rodrigues T, Borges P, Mar L, Marques D, Albano M, Eickhoff H, Carrelo C, Almeida B, Pires S, Abrantes M, Martins B (2020) GLP-1 improves adipose tissue glyoxalase activity and capillarization improving insulin sensitivity in type 2 diabetes. Pharmacol Res Commun 1(161):105198

Sachdeva AK, Kuhad A, Chopra K (2014) Naringin ameliorates memory deficits in experimental paradigm of Alzheimer's disease by attenuating mitochondrial dysfunction. Pharmacol Biochem Behav 1(127):101–110

Sajad M, Kumar R, Thakur SC (2022) History in Perspective: The prime pathological players and role of phytochemicals in Alzheimer's disease. IBRO Neurosci Rep 1(12):377–389

Salkovic-Petrisic M, Knezovic A, Hoyer S, Riederer P (2013) What have we learned from the streptozotocin-induced animal model of sporadic Alzheimer's disease, about the therapeutic strategies in Alzheimer's research. J Neural Transm 120:233–252

Sanchez-Rodriguez D, Gonzalez-Figueroa I, Alvarez-Berríos MP (2023) Chaperone activity and protective effect against Aβ-induced cytotoxicity of artocarpus camansi blanco and amaranthus dubius mart. ex thell seed protein extracts. Pharm 16(6):820

Shah P, Chavda V, Patel S, Bhadada S, Ashraf GM (2020) Promising anti-stroke signature of Voglibose: investigation through in-silico molecular docking and virtual screening in in-vivo animal studies. Curr Gene Ther 20(3):223–235

Sharma P, Singh R (2012) Dichlorvos and lindane induced oxidative stress in rat brain: protective effects of ginger. Pharmacognosy Res 4(1):27

Sharma S, Taliyan R (2015) Synergistic effects of GSK-3β and HDAC inhibitors in intracerebroventricular streptozotocin-induced cognitive deficits in rats. Naunyn-Schmiede Arch Pharmacol 388:337–349

Singh L, Singh S (2023) Neuroprotective potential of Honokiol in ICV-STZ induced neuroinflammation, Aβ (1–4 2) and NF-kB expression in experimental model of rats. Neurosci Lett 16(799):137090

Sottocasa GL, Kuylenstierna BO, Ernster L, Bergstrand A (1967) An electron-transport system associated with the outer membrane of liver mitochondria: a biochemical and morphological study. J Cell Biol 32(2):415–438

Tezel G (2022) Molecular regulation of neuroinflammation in glaucoma: Current knowledge and the ongoing search for new treatment targets. Prog Retin Eye Res 1(87):100998

Tirichen H, Yaigoub H, Xu W, Wu C, Li R, Li Y (2021) Mitochondrial reactive oxygen species and their contribution in chronic kidney disease progression through oxidative stress. Front Physiol 23(12):398

Wang D, Gao K, Li X, Shen X, Zhang X, Ma C, Qin C, Zhang L (2012a) Long-term naringin consumption reverses a glucose uptake defect and improves cognitive deficits in a mouse model of Alzheimer's disease. Pharmacol Biochem Behav 102(1):13–20

Wang SW, Wang YJ, Su YJ, Zhou WW, Yang SG, Zhang R, Zhao M, Li YN, Zhang ZP, Zhan DW, Liu RT (2012b) Rutin inhibits β-amyloid aggregation and cytotoxicity, attenuates oxidative stress, and decreases the production of nitric oxide and proinflammatory cytokines. Neurotoxicol 33(3):482–490

Wills E (1966) Mechanisms of lipid peroxide formation in animal tissues. Biochem J 99(3):667

Xue P, Zz L, Gg J, Lp W, Cm B, Yl W, Chen MF, Li W (2022) The role of LRP1 in Aβ efflux transport across the blood-brain barrier and cognitive dysfunction in diabetes mellitus. Neurochem Int 1(160):105417

Yamini P, Ray RS, Chopra K (2018) Vitamin D 3 attenuates cognitive deficits and neuroinflammatory responses in ICV-STZ induced sporadic Alzheimer's disease. Inflammopharmacol 26:39–55

Yamini P, Ray RS, Yadav S, Dhaliwal J, Yadav M, Kondepudi KK, Chopra K (2022) α7nAChR activation protects against oxidative stress, neuroinflammation and central insulin resistance in ICV-STZ induced sporadic Alzheimer's disease. Pharmacol Biochem Behav 1(217):173402